Vertical and Relaxed Structures of a Reactive Organosilane Radical Cation from CW and Transient Resonance Raman Spectra

Jerry T. Godbout,[†] Matthew D. Pietrzykowski,[†] Ian R. Gould,[†,#] Joshua L. Goodman,[†] and Anne Myers Kelley*[,†]

Department of Chemistry and Center for Photoinduced Charge Transfer, University of Rochester, Rochester, New York 14627-0216, and Research Laboratories, Eastman Kodak Company, Rochester, New York 14650-2109

Received: January 28, 1999; In Final Form: March 25, 1999

Resonance Raman spectra of two *p*-methoxybenzyltrialkylsilanes (alkyl = methyl and ethyl) have been obtained both as their neutral charge-transfer complexes with tetracyanoethylene in steady-state cw experiments and as their radical cations via two-color pump−probe transient measurements. The ground-state charge-transfer resonant spectra exhibit intensity predominantly in phenyl-localized modes, suggesting that vertical excitation to the contact ion-pair state involves little participation of the bond that is known to undergo subsequent nucleophile-assisted cleavage in the separated radical cation. Quantitative modeling of the absolute cross sections for the methyl compound is used to determine the mode-specific reorganization energies accompanying vertical electron transfer. Transient spectra of the relaxed radical cations show more than 20 resonance-enhanced modes, several of which have significant contributions from the C−Si stretching coordinate based on frequency shifts between the natural abundance and benzyl ^{13}C labeled methyl compounds. These modes with significant benzyl C−Si stretching character are considerably lower in frequency in the radical cation than in the neutral, indicating weakening of this bond upon oxidation. The experimental frequencies are reproduced quite well by density functional theory calculations at the B3LYP/6-31g(d,p) level which give a C−Si bond length increase of 0.10 Å upon oxidation.

Introduction

The use of resonance Raman spectroscopy as a probe of structural changes in electronically excited molecules has long been established.[1,2] A variety of recent studies have employed resonance Raman intensity analysis to elucidate the structural changes caused by electron transfer in both noncovalent charge-transfer (CT) complexes and covalent systems having CT electronic transitions.[3] Both vibrational mode-specific reorganization energies and, in some cases, extrapolated relaxed geometries of the ion-pair states have been obtained. The main goal of this previous work has been to test and extend the current theories for electron transfer rates, and efforts have been made to completely describe all of the radiative and nonradiative processes associated with electron transfer using a "unified theory" and a common set of reorganization parameters.

The most appropriate systems for such fundamental studies of electron transfer theories are essentially unreactive chemically. However, in many applications of photoinduced electron transfer, utilization of the chemical potential energy of the ion-pair state to initiate a useful chemical reaction is the ultimate goal. Electron transfer in neutral organic molecules results in the formation of radical anions and radical cations. The reactions of photochemically produced organic radical ions have been the subject of a large number of investigations. A particularly useful reaction of an organic radical ion is fragmentation to form a neutral radical and an anion or cation (which may be a proton), since these are catalytic species that may find use in a wide variety of applications. Traditionally, these reactions have been studied using product analysis, quantum efficiency and absolute rate measurements, and, in some cases, thermodynamic measurements. In principle, vibrational spectroscopy should also be very informative in studies of bond-breaking processes. Although vibrational spectra of a number of organic radical ions have been measured, both in low-temperature matrices[4−6] and in room temperature solutions,[7−13] to the best of our knowledge no studies have been performed on radical ions that actually undergo efficient fragmentation or any other useful chemical reaction. The main idea behind this work, then, is to apply the resonance Raman spectroscopic methodologies for charge-transfer states discussed above to useful chemically reacting systems.

The systems chosen for study are the radical cations of the benzyltrialkylsilanes **1** and **2**:

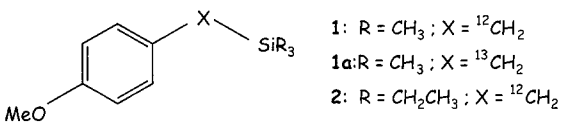

These species undergo facile cleavage of the C−Si bond via a nucleophilic S_N2 mechanism.[14] The silanes are sufficiently reactive that the nucleophile may be the solvent or impurities in the solvent. An interesting question concerns the extent to which the radical cation initially formed by direct electronic

* Corresponding author. Tel. 785-532-6665. Fax 785-532-6666. E-mail: amKelley@ksu.edu. Current address: Department of Chemistry, Kansas State University, 112 Willard Hall, Manhattan, KS 66506-3701.

[†] University of Rochester.

[#] Eastman Kodak Co. and Center for Photoinduced Charge Transfer, University of Rochester. Current address: Department of Chemistry and Biochemistry, Arizona State University, Tempe, Arizona 85287.

10.1021/jp990339b CCC: $18.00
Published on Web 05/01/1999

excitation of a charge-transfer complex is the "same" species that undergoes the subsequent reaction. Direct excitation of a charge-transfer absorption is expected to involve primarily the molecular orbitals on the aromatic ring; does this phenyl-centered ion radical then evolve to a species having more positive charge on the Si through an electronic radiationless transition and/or vibrational or solvent relaxation?

We address this question by carrying out resonance Raman studies of two different types. In the first experiment, an electron donor D (one of the silanes of interest) and an electron acceptor A (tetracyanoethylene, TCNE) form a ground-state complex, DA. Photoexcitation of the charge-transfer (CT) absorption band of the complex corresponds to electron transfer from donor to acceptor—that is, the excited electronic state of the complex is the radical ion pair, $D^{\bullet+}/A^{\bullet-}$. The CT-resonant Raman spectrum therefore exhibits the frequencies of the neutral DA complex, but intensities that depend on the differences in potential energy surfaces between DA and the vertically excited ion pair, $D^{\bullet+}/A^{\bullet-}$. A recent review summarizes related studies on both CT complexes and covalently bonded donor−acceptor molecules.[3] The separated, vibrationally relaxed radical ions could, however, have very different structures from the vertically excited charge-transfer complex due to structural relaxation along anharmonic coordinates, solvent reorganization, and/or conversion to a different electronic state. Therefore, a second experiment directly measures the vibrational frequencies of the relaxed $D^{\bullet+}$ radical cation by pump−probe Raman spectroscopy on resonance with a transient absorption of $D^{\bullet+}$. While both ground-state resonance Raman intensity analysis and pump−probe Raman spectroscopy of transient species are well-developed techniques, there exist only a few examples (e.g. the S_1 state of *trans*-stilbene)[15−20] where both experiments have been performed on the same molecule, and none, to our knowledge, where the product of an electron-transfer reaction has been probed in both ways.

The present work has several main goals. We wish to explore the utility of vibrational spectroscopy in studies of the chemical reactions of organic radical ions, and to extend the previous ground-state resonance Raman intensity analyses of charge-transfer complexes by comparing data with pump−probe Raman spectroscopic studies on the same system, thus obtaining information regarding relaxation effects in an organic radical cation formed by photooxidation. Finally, the vibrational spectra of the silanes are considerably more complex than those of the simpler unreactive systems studied previously by us, and assignment of the important features of the spectrum required the use of electronic structure calculations, as described recently by others.[12,21] This work thus also adds to the comparisons between experiment and theory in vibrational studies of charge-transfer systems.

Experimental and Computational Methods

Tetracyanoethylene was obtained from Aldrich and sublimed under vacuum three times before use. The sensitizer, 3,3′,4,4′-benzophenonetetracarboxylic dianhydride (BTDA), was obtained from Aldrich and recrystallized several times from 10:1 benzene: acetic anhydride and vacuum-dried overnight. The silanes **1** and **2** were synthesized via Grignard coupling using methods described previously.[14,22] **1a** was synthesized in a similar fashion using 4-methoxybenzyl chloride with ^{13}C substitution at the benzyl position as a starting material. GC-MS and ^1H NMR indicate an isotopic purity of 99%. The model compounds benzyltrimethylsilane and 4-methylanisole were used as purchased from Aldrich, and 4-ethylanisole was a gift from Professor J. P. Dinnocenzo.

Charge-transfer complexes of **1, 1a**, and **2** with TCNE were made by mixing solutions of the donor and acceptor in spectroscopic grade dichloromethane. The absorption spectra consist of two broad bands centered near 400 and 620 nm. Neither band is present in the donor or acceptor alone and so both presumably correspond to charge-transfer excitations, but we have made no effort to characterize the bluer absorption band. In this study, the 620 nm transition was excited exclusively; due to the large energy spacing and the lower intensity of the higher-energy transitions, contributions from the higher-energy state to the Raman enhancement are considered to be negligible.[23] The Benesi−Hildebrand method[24−26] was used to determine the equilibrium constant K_{eq} and molar absorptivity ϵ for the longer-wavelength absorption band of the **1**:TCNE complex. Solutions were prepared at excess donor concentrations of 33−199 mM and a constant acceptor concentration of 1.5 mM. Absorption spectra were measured on a Perkin-Elmer Lambda 19 UV−vis spectrophotometer in a 1 cm path length cell thermostated at 25 °C. The ratio $[TCNE]_0/A$, where $[TCNE]_0$ is the initial (stoichiometric) TCNE concentration and A is the absorbance at the CT band maximum, was plotted versus the reciprocal donor concentration, 1/[D], and fit to the Benesi−Hildebrand equation:

$$\frac{[TCNE]_0}{A} = \frac{1}{K_{eq}\epsilon}\frac{1}{[D]} + \frac{1}{\epsilon} \qquad (1)$$

This form of the equation is appropriate when the donor is in large excess and only 1:1 complexes are important. The possibility of 2:1 (DAD or DDA) complexes cannot be ruled out, but we observed no evidence for such complexes (e.g. the absorption spectral band shapes appeared independent of donor concentration over a wide range).

Resonance Raman spectra of the charge-transfer complexes were obtained using the general setup described previously[27−29] except that a backscattering geometry was employed with the rotating cell. Tunable excitation was provided by a CW argon-pumped dye laser operating with either Rhodamine 590 or DCM with about 20 mW of power at the sample. The solutions were made to be 30 mM in both donor and acceptor, resulting in a final complex concentration of about 1 mM. Spectra of 30 mM donor alone and 30 mM acceptor alone in dichloromethane were also measured to allow subtraction of the nonresonant Raman background arising from the uncomplexed donor and acceptor present in the solutions. Absorption spectra taken at the beginning and the end of the Raman experiments were nearly identical (often the absorbances increased slightly due to some evaporation of the volatile solvent), indicating little or no photochemical degradation of the samples during ca. 60 min of data accumulation. The spectra were calibrated in frequency using known solvent lines as a reference. Intensities were corrected for reabsorption and for the wavelength dependence of the detector sensitivity using a quartz-halogen tungsten filament lamp (Optronics model 245C).[2,30] Finally, integrated band areas were determined by subtracting a linear or quadratic baseline and fitting regions of the spectra to sums of Voigt line shapes using the LabCalc or Origin software packages. Displayed spectra have been spliced together using bands appearing in both windows for normalization.

Absolute cross sections were determined by using the 702/740 cm^{-1} doublet of CH_2Cl_2 as an internal standard.[2] The cross section for this doublet was in turn determined by measuring its intensity (differential cross section at 90°, both polarizations)

relative to that of the 802 cm^{-1} line of cyclohexane and the 993 cm^{-1} line of benzene as external standards,[31] as well as by using the 802 cm^{-1} line of cyclohexane as an internal standard in mixtures of equal volumes of CH_2Cl_2 and cyclohexane. While the cross section of methylene chloride in cyclohexane is not necessarily identical to that of neat methylene chloride, the internal standard method has the advantage of eliminating errors due to imperfect matching or positioning of the cuvettes and drifts in laser power, and we observed no systematic differences between the two methods.

Nonresonant Raman spectra of neat liquids were obtained on the same instrument with the samples contained in stationary glass capillaries. The samples were excited with the 514.5 nm line from a CW argon ion laser.

Resonance Raman spectra of the radical cations of **1**, **1a**, and **2** in acetonitrile were acquired using an electron-transfer sensitization method.[32,33] Excitation of BTDA (ca. 20 mM) with the third harmonic (355 nm, 0.26 mJ/pulse) of a Q-switched Nd:YAG laser (Spectra-Physics GCR 150−30) results in formation of the BTDA excited triplet state, ^{3}BTDA*.[34] Quenching of the ^{3}BTDA* by the silanes occurs via diffusion-controlled electron transfer to give a triplet BTDA radical anion/silane radical cation pair.[34] As described previously, spin-forbidden return electron transfer within the triplet radical-ion pair to regenerate neutral reactants is inefficient, and rapid separation of the radical-ion pair occurs withinin ca. 5 ns in acetonitrile to generate two separated noninteracting radical ions, each in a doublet spin state.[33] The Raman spectra of the silane radical cations were obtained using a nanosecond probe pulse from the same laser (532 nm, 0.13 mJ/pulse, ca. 1 mm focused beam diameter), delayed by 35 ns. The excitation and probe beams were recombined using a dichroic beam splitter and focused into the sample, contained in a stirred 1 cm fused silica cuvette. Assuming a molar absorptivity of ca. 10 000 M^{-1} cm^{-1} for the silane radical cation, the energy density in the probe pulse should be sufficient to excite a large fraction of the radical cations in the probed volume and substantially deplete the ground-state radical cation population if its excited-state lifetime is not short relative to the ca. 8 ns pulse duration. While we cannot be certain that none of the features in our pump−probe spectra arise from higher excited states or photoproducts, such species are unlikely to be seen in the resonance Raman unless they happen to have strong absorbances at the probe wavelength. The Raman scattering was collected in backscattering geometry, focused with a fused silica lens, and passed through a quartz polarization scrambler before being dispersed by a Spex 500M 0.5 m single-stage spectrograph. A holographic supernotch filter (Kaiser Optical Systems) was used to reject scattered laser light. The Raman scattered light was detected with a Princeton Applied Research (PAR) 1461 intensified photodiode array operating at approximately −30 °C. A PAR 1302 fast pulser was used to gate the detector (20 ns window) with the probe pulse in order to discriminate against fluorescence induced by the pump pulse.

The resonance Raman and absorption spectra were modeled using the time-dependent formalism described in detail elsewhere.[2,3,27] DFT calculations were performed using Gaussian 94.[35] Geometry optimizations and frequency calculations were done with the B3LYP hybrid density functional and the 6-31g-(d,p) basis set. The ^{13}C frequency shifts were calculated from the force constants obtained from the Gaussian 94 results using the processing utility Gar2ped.[36] The normal modes were visualized using XMol 1.3.1.[37]

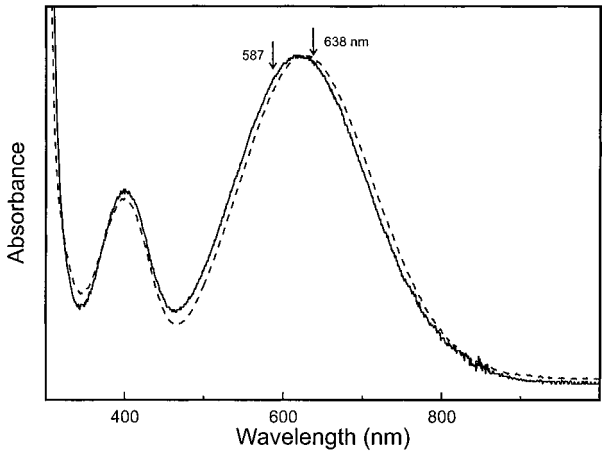

Figure 1. Absorption spectra of complexes of **1** (solid) and **2** (dashed) with TCNE in methylene chloride. Arrows indicate Raman excitation wavelengths.

Results

Figure 1 shows the absorption spectra of the **1**:TCNE and **2**:TCNE complexes. Benesi−Hildebrand analysis of the **1**:TCNE complex in methylene chloride at 25 °C gives an equilibrium constant of K_{eq} = [complex]/{[donor][TCNE]} = 1.1 ± 0.2 M^{-1} and a peak molar absorptivity of ϵ = 1900 ± 200 M^{-1} cm^{-1}. Estimated error limits are based on the reproducibility of the values among independent runs performed on different days in somewhat different donor concentration ranges. For comparison, Frey and co-workers report K_{eq} = 0.98 ± 0.10 M^{-1} and ϵ = 1350 ± 130 M^{-1} cm^{-1} for the related complex, 4-methylanisole:TCNE in methylene chloride at 22 °C.[38]

After dividing by the ω^4 prefactor, the differential Raman cross section of the 702/740 cm^{-1} doublet of CH_2Cl_2 was found to be constant to within experimental uncertainty between 457.9 and 700 nm; that is, no preresonance enhancement was observed in the visible frequency region. Our final average value for the differential cross section is

$$(d\sigma/d\Omega)_{\parallel+\perp} = 7.52 \times 10^{-31}\, \varpi^3_{scatt}\varpi_{laser} \qquad (2)$$

where ϖ_{scatt} and ϖ_{laser} are the laser and scattered wavenumbers in cm^{-1}, and the resulting cross section has units of $Å^2$ $molecule^{-1}$ sr^{-1}. There are at least two prior literature values for this cross section: Nestor and Lippincott report 1.15 × 10^{-15} $Å^2$ $molecule^{-1}$ sr^{-1} at 488 nm[39] compared with our value from eq 2 of 1.19 × 10^{-15}, and Eysel and Bertie obtain (after converting their reported scattering activity into a differential cross section) 1.03 × 10^{-15} $Å^2$ $molecule^{-1}$ sr^{-1} at 514.5 nm[40] compared with the eq 2 value of 9.6 × 10^{-16}. The agreement appears good, although it is not clear whether the previously reported cross sections refer to the stronger 702 cm^{-1} line alone or to the combined 702/740 cm^{-1} doublet as ours do.

The resonance Raman spectra obtained from the complexes of **1** and **2** with TCNE are shown in Figures 2 and 3. Five lines clearly exhibit some degree of resonance enhancement in the **1**/TCNE spectrum relative to the pure donor and pure acceptor spectra. The lines at 2227/2238 and 1554 cm^{-1} correspond to vibrations of TCNE that are also resonance enhanced in the hexamethylbenzene/TCNE complex,[27] while the lines at 1604, 1211, and 1177 cm^{-1} correspond closely to nonresonant Raman lines of neat **1** and are assigned as resonance-enhanced donor-localized vibrations. The assignments of these donor vibrations given in Table 1 are based on comparison with nonresonant Raman spectra of the model compounds benzyltrimethylsilane,

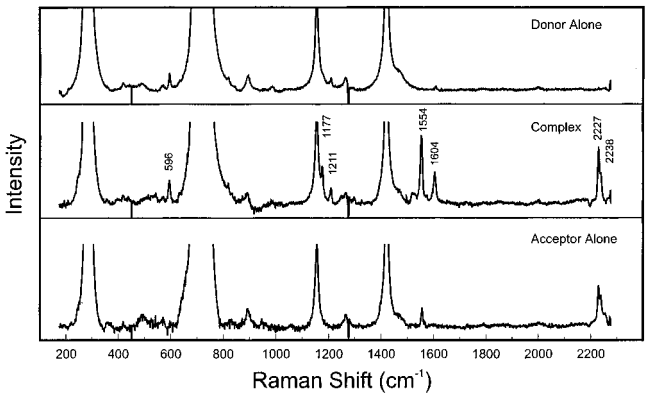

Figure 2. Raman spectra of 30 mM **1** (top), 30 mM **1** + 30 mM TCNE (middle), and 30 mM TCNE (bottom) in methylene chloride taken with 587 nm excitation (20 mW). Each spectrum is a sum of 30 accumulations of 120 s each. Labeled frequencies indicate resonance-enhanced transitions of the donor/acceptor complex; strong lines are due to solvent.

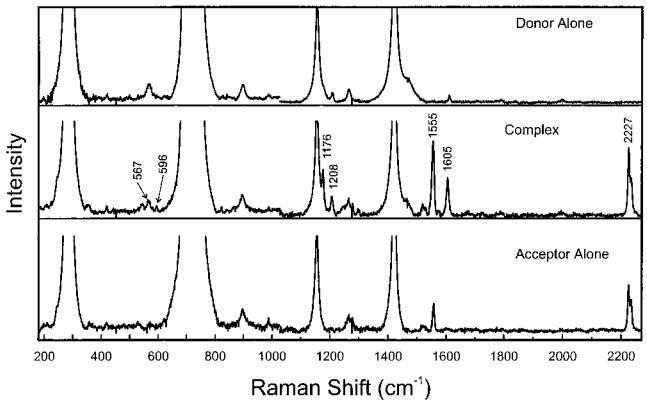

Figure 3. Raman spectra of 30 mM **2** (top), 30 mM **2** + 30 mM TCNE (middle), and 30 mM TCNE (bottom) in methylene chloride with 638 nm excitation (20 mW). Each spectrum is a sum of 60 accumulations of 60 s each. Labeled frequencies indicate resonance-enhanced transitions of the donor/acceptor complex; strong lines are due to solvent.

4-methylanisole, and 4-ethylanisole, published assignments for 4-methylanisole,[41] and our density functional calculations on **1**. The two strongest donor-localized lines (1604 and 1177 cm^{-1}) shift by no more than 2 cm^{-1} between **1** and **1a** and are clearly assigned to ring modes having little or no contribution from the $Si-CH_2$ stretch. The weaker 1211 cm^{-1} band, which exhibits a large shift of 8 cm^{-1} in **1a**, is assigned as principally the $Ph-CH_2$ stretch. A significant contribution of $Si-CH_2$ stretching to this normal mode seems to be ruled out by the observation that not only **1** and **2** but also 4-methylanisole and 4-ethylanisole, which lack the silane group entirely, all show a fairly strong nonresonant Raman line between 1203 and 1211 cm^{-1}. In addition, a band is observed at 596 cm^{-1} in the **1**/TCNE spectrum. Both neat **1** and pure TCNE have Raman bands at 596 cm^{-1} (it is the strongest Raman line in neat **1**), while the corresponding mode in neat **2** appears at 563 cm^{-1}. The frequency and intensity of this line suggest that it should be assigned to C−Si "symmetric stretching" by comparison with previous assignments for trimethylvinylsilane,[42] while our density functional calculations suggest that the motion is predominantly stretching of $Si-CH_3$ bonds with a smaller contribution from $Si-CH_2$ stretching. The resonance Raman spectrum of the **2**/TCNE complex, shown in Figure 3, exhibits bands of fairly comparable intensity at both 563 and 596 cm^{-1}, indicating that the 596 cm^{-1} feature in the **1**/TCNE complex has contributions from both the silane and TCNE. In both

TABLE 1: Experimental and Calculated Resonance Raman Intensities[a] of 1/TCNE Complex in CH_2Cl_2

Raman shift (cm^{-1})	assignment[b]	cross section (Å²/molecule × 10^{12}) 587 nm expt	587 nm calc	638 nm expt	638 nm calc	Δ	λ (cm^{-1})[c]
595[d]	$Si-(CH_3)_3$ sym str	7.3	8.0	8.6	7.9	0.445	59
597[d]	TCNE	7.3	8.0	8.6	8.0	0.445	59
1177	Ph 9a	64	69	62	63	0.67	260
1211	$Ph-CH_2$ str	14	21	32	19	0.36	78
1554	TCNE	270	280	220	240	1.05	860
1604	Ph 8a	130	140	120	120	0.72	420
2227	TCNE	110	110	60	80	0.485	260
2238	TCNE	15	15	*e*	11	0.18	36

[a] Other parameters used in fit: transition length $\mu = 0.595$ Å; electronic zero-zero energy $E_0 = 11\,700$ cm^{-1}; inhomogeneous Gaussian standard deviation = 200 cm^{-1}; homogeneous fwhm $\Gamma = 2500$ cm^{-1}; line-shape parameter for Brownian oscillator solvent broadening function $\kappa = 0.1$. These values of κ and Γ correspond to a solvent reorganization energy of 2820 cm^{-1}. See refs 27 and 28 for explanation of parameters. [b] Phenyl-localized modes are denoted using the convention of Varsanyi.[41] [c] Reorganization energy given by $\lambda = \omega\Delta^2/2$. [d] Intensity of overlapping lines assigned to equal contributions from near-degenerate donor and acceptor vibrations (see text). [e] Not accurately measurable after subtraction of the nonresonant contribution.

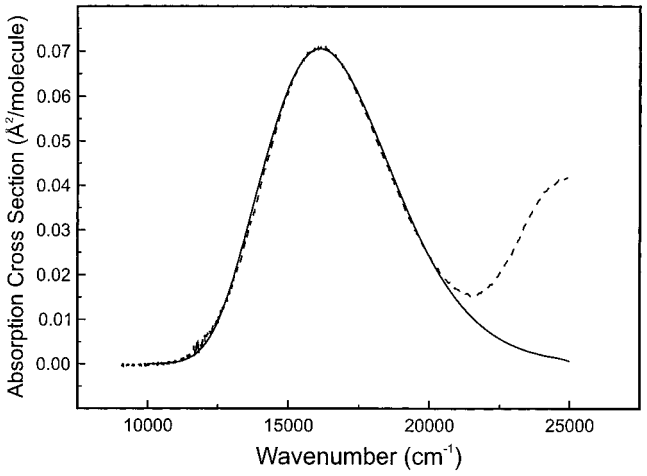

Figure 4. Experimental absorption spectrum of **1**/TCNE complex in methylene chloride (dashed) and spectrum calculated from parameters from Table 1 (solid).

complexes, however, the resonance enhancement is minimal, with much of the intensity in the **1**/TCNE spectrum actually arising from uncomplexed donor. For the purposes of spectral modeling, the intensity at 596 cm^{-1} in the **1**/TCNE spectrum was assigned to equal contributions from a donor mode and an acceptor mode nearly degenerate in frequency.

The results of the Raman spectral modeling are compiled in Table 1. The calculated resonance Raman intensities are very similar at 587 and 638 nm, as expected in view of the comparable absorbances at these two wavelengths. The experimental intensities are also quite similar at both excitation frequencies with the exception of the 1211 and 2238 cm^{-1} lines; we have no explanation for this discrepancy, and suspect that much or all of it may simply be experimental uncertainty in these lines that show relatively weak resonance enhancement and require subtraction of large nonresonant scattering contributions from the uncomplexed donor and acceptor. The absorption spectrum generated from the same parameters is compared with the experimentally observed spectrum in Figure 4.

The resonance Raman spectra of the radical cations of **1**, **1a**, and **2** are presented in Figures 5 and 6. The nonresonant Raman

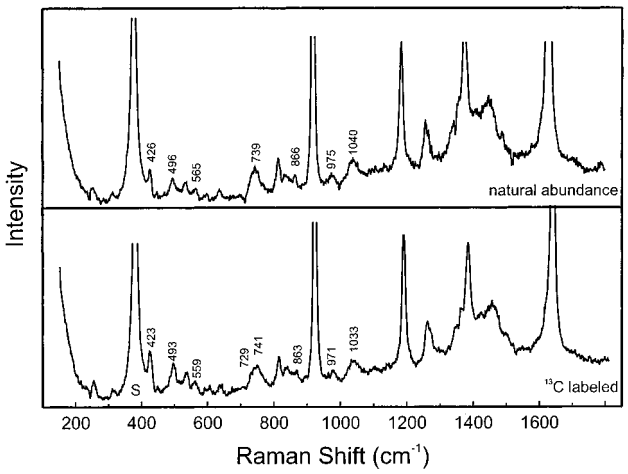

Figure 5. Pump−probe resonance Raman spectra of 20 mM **1** (top) and 20 mM **1a** (bottom) in acetonitrile solvent with 20 mM BTDA as a cosensitizer. Displayed spectra have been pieced together from three separate detection windows, each a sum of ten 60 s accumulations. Labeled frequencies indicate Raman lines of the **1** radical cation that are shifted by more than 2 cm^{-1} upon isotopic substitution. Peaks marked S are due to nonresonant solvent scattering.

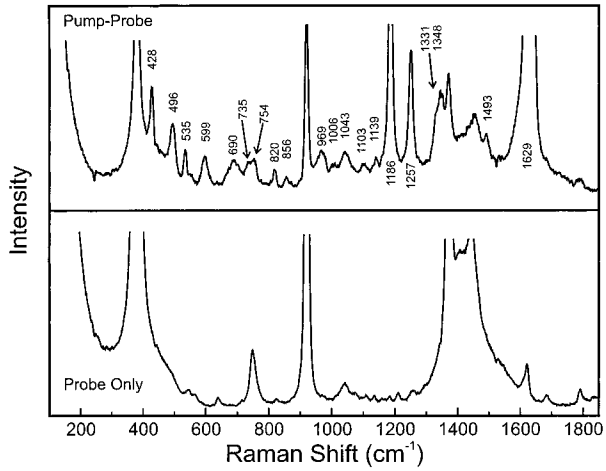

Figure 6. Pump−probe (top) and probe-only (bottom) resonance Raman spectra of 20 mM **2** in acetonitrile solvent with 20 mM BTDA as a cosensitizer. Displayed spectra have been pieced together from three separate detection windows, each a sum of ten 60 s accumulations. Labeled frequencies indicate Raman lines of the **2** radical cation. The probe-only spectrum is dominated by solvent lines.

spectra of neat **1** and **1a** are shown for comparison in Figure 7. The transient spectra are intense and show more than 20 Raman bands that can be attributed to the radical cation. The interesting observables in this experiment are not the Raman intensities but the vibrational frequencies, which provide information on the equilibrium geometry and force constants of the "relaxed" radical cation. It is not clear in general how to assign frequencies of the neutral and the radical ion to corresponding vibrational modes, but the spectra of the isotopically substituted silane do allow identification of modes involving significant motion of the benzylic carbon. Table 2 lists the Raman bands of both the radical cation and the neutral that shift upon benzyl ^{13}C substitution, suggesting a contribution from the chemically interesting benzyl C−Si stretching coordinate. The distribution of the isotopic shift among 7−8 observed vibrations suggests that the C−Si stretch is delocalized over a number of normal modes, although predominantly phenyl-C stretching modes and

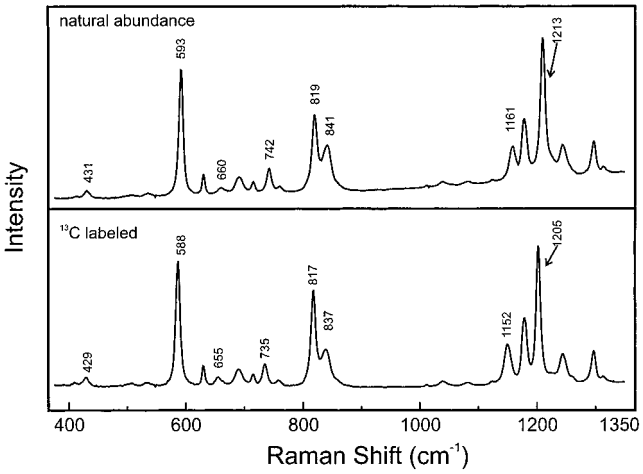

Figure 7. Nonresonant Raman spectra of neat **1** and **1a** taken with 514.5 nm excitation. Frequencies shifted by more than 2 cm^{-1} upon isotopic substitution are labeled.

TABLE 2: Experimental Frequencies of Neutral and Radical Cation Forms of 1 and 1a[a]

neutral freq (cm^{-1})[b]		radical cation freq (cm^{-1})[c]	
natural abund	^{13}C	natural abund	^{13}C
431	429	426	423
593	588	496	493
660	655	565	559
742	735	739	729/741
819	817	866	863
841	837	975	971
1161	1152	1040	1033
1213	1205		

[a] All shifts greater than 2 cm^{-1} are listed. [b] Nonresonant Raman, neat. [c] Resonant Raman pump−probe in solution.

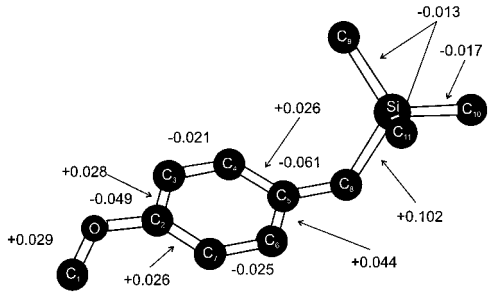

Figure 8. Calculated bond length changes [B3LYP/6-31g(d,p)] between the equilibrium geometries of **1** and its radical cation (cation bond length minus neutral bond length). The C−H bond lengths change by no more than 0.01 Å. The principal bond angle changes (those exceeding 1°) are C_1-O-C_2, +3.4°; C_5-C_8-Si, −1.6°; $H-C_8-H$, +4.8°; C_9-Si-C_{10} and $C_{10}-Si-C_{11}$, +2.9°; C_9-Si-C_{11}, +2.6°.

bending modes involving the benzyl carbon should also shift upon benzyl ^{13}C substitution.

The DFT calculations provide additional assistance in assigning the vibrations as well as allowing direct comparison of experimental and calculated frequencies. The calculated changes in equilibrium geometry between **1** and its radical cation are shown in Figure 8. Although most of the bond lengths change to some extent, the greatest changes involve the CH_2-Si and CH_2-phenyl bonds. The calculated normal modes of the neutral and radical cation were then compared by visual inspection of the animated vibrations to determine the best correspondence between modes of the two species. Table 3 shows this correspondence for the calculated vibrations that exhibit significant isotopic shifts, along with the comparison between

TABLE 3: Calculated and Experimental ^{13}C Frequency Shifts for Neutral and Radical Cation Forms of 1 and 1a[a]

neutral				radical cation				
calc		expt		calc		expt		
freq	^{13}C shift	freq	^{13}C shift	freq	^{13}C shift	freq	^{13}C shift	mode description[b]
				361	−3			CH_2-Ph ip bend, Ph ip def
				428	−3	426	−3	Ph 6a, Ph−CH_2−Si bend
661	−5	660	−5	478	−6	496	−3	CH_2−Si str, Si−$(CH_3)_3$ def
				538	−3			ip Ph def, Ph−CH_2−Si bend, Ph−O−CH_3 bend
				554	−3	565	−6	Ph 16b, CH_2−Si−CH_3 str
690	−4			724	−3			Si−CH_3 asym str, Si−CH_3 rocks, CH_2 twist
584	−4	593	−5	748	−4	739	−10/+2	Si−CH_3 sym str, ring def, Si−CH_2 str
832	−4	841	−4	829	−4			CH_2 and CH_3 defs
752	−8	742	−7	830	−3			Ph−CH_2 str, Ph breathe[c]
1199	−8	1161	−9	1073	−6	1040	−7	CH_2 ip rock, CH_2−Si str
1235	−9	1213	−8	1288	−5			Ph−CH_2 str
1465	−3			1489	−6			CH_2 scissor

[a] Frequencies in cm^{-1}. All calculated modes with ^{13}C shifts ≥ 2.5 cm^{-1} are listed. [b] Mode descriptions and correlations between modes of neutral and cation are qualitative and based on visual examination of the animated modes. ip = "in-plane", op = "out-of-plane", def = deformation, str = stretch. Phenyl-localized modes are denoted using the convention of Varsanyi.[41] [c] Particularly poor correspondence between neutral and cation modes.

calculated and observed frequencies. The frequency comparison between the neutral species and the radical cations is only slightly compromised by the fact that the former were measured in the neat liquids and the latter in acetonitrile solution, since solvent shifts are typically less than 5 cm^{-1} for solutes of this type. Because of the differences in both equilibrium geometries and force constants, the normal modes of the neutral and the radical cation have different forms and "corresponding" modes of the two species cannot be unambiguously defined. However, the two modes having the greatest degree of Si−CH_2 stretching character are calculated to shift to considerably lower frequencies in the radical cation (661 and 1199 cm^{-1} in the neutral versus 478 and 1073 cm^{-1} in the radical cation) while the modes having the greatest degree of Ph−CH_2 stretching character are calculated to shift to somewhat higher frequencies (752 and 1235 cm^{-1} versus 830 and 1288 cm^{-1}), consistent with the predicted lengthening of the Si−CH_2 bond and shortening of the Ph−CH_2 bond in the cation. All four Si−CH_2 stretching frequencies correspond reasonably well to experimental frequencies having about the expected isotopic shifts, but unfortunately the prediction for the Ph−CH_2 stretching modes cannot be verified experimentally since these modes do not seem to have intensity in the radical cation spectrum.

Discussion

The reorganization parameters presented in Table 1 must be considered approximate due to the weakness of the spectra, the correspondingly large uncertainties in the experimental cross sections, and the availability of data at only two excitation frequencies. The strong solvent scattering may also obscure other resonance-enhanced modes of the donor, including the 660 cm^{-1} mode assigned to predominantly Si−CH_2 stretching and observed as a weak line in the nonresonant spectrum of neat **1**. Nevertheless, the observation of mainly phenyl-localized modes in the resonance Raman spectra of the charge-transfer complex does seem to indicate that the electron is removed mainly from the π system of the phenyl ring, and that the hole remains there for at least a few vibrational periods. The charge-transfer absorption maximum of **1**/TCNE (620 nm) is only 0.2 eV lower in energy than the corresponding band of a model compound lacking the silyl group, 4-ethylanisole/TCNE (563 nm), also indicating that the vertical charge-transfer excitation is largely (but not entirely) phenyl-localized. The chemistry of these silane radical cations, however, is that it is the C−Si bond that undergoes cleavage. This suggests that the charge distribution, and with it the geometry, undergoes some change on a time scale of tens of femtoseconds to nanoseconds following oxidation. The results of the DFT calculation also show that the structure of the relaxed radical cation differs from that of the neutral predominantly at the silyl group end, and involves significant lengthening of the benzyl C−Si bond with a concomitant shortening of the C−phenyl bond.

Quantitative comparison between the results of the steady-state and transient Raman experiments is hindered by fundamental differences in the kind of information the two experiments provide. The resonance Raman intensities in the ground state CT-resonant experiment are determined predominantly by the local slope of the excited state (CT) potential energy surface near the ground state (neutral) geometry. This slope (first derivative of the potential) is dominated by the displacement between the potential minima of the two surfaces (the Δ parameter in the spectral fitting) and not by the change in local vibrational frequency, which appears only in the second derivative. Usually, and certainly in this case, the intensities simply are not sensitive enough to frequency changes to allow both the displacement and the excited-state frequency to be determined with any confidence, and all of the intensity is attributed to the displacement (change in equilibrium bond length for a stretching vibration). The transient experiment, on the other hand, measures directly only the vibrational frequency of the ion. While a reduced frequency for a stretching mode almost always corresponds to a longer bond, the empirical correlations quantitatively relating the two (e.g. Badger's rule)[43−46] hold only for particular bonds within given classes of molecules and cannot be readily generalized. Finally, chemical reactivity depends on the bond dissociation energy, which in turn is only indirectly related to the vibrational frequency near the bottom of the well.

An obvious question is what CT-resonant Raman intensity would be predicted if the DFT-calculated C−Si bond length change were "felt" immediately in the vertically excited state. If there were a normal mode describable as a pure quasidiatomic C−Si stretch, the calculated bond length change of 0.102 Å in a mode at about 600 cm^{-1} would correspond to a dimensionless displacement of $\Delta \sim 1.3$. This is considerably larger than that

found from the resonance Raman intensity analysis for any single normal mode of the donor (since resonance Raman intensities are roughly proportional to Δ^2, a mode with $\Delta = 1.3$ would be about 9 times as intense as one having the same frequency and $\Delta = 0.445$). However, the DFT calculations also predict that the benzyl C−Si stretch is actually distributed over at least three principal normal modes (595, 660, and 1161 cm^{-1}, see Table 3), with smaller contributions to a number of others. The intensity of the 595 cm^{-1} donor line is quite uncertain due to its accidental near-degeneracy with a TCNE line, the 660 cm^{-1} line would be entirely buried under the very strong 702 cm^{-1} solvent band, and the 1161 cm^{-1} line would be strongly overlapped by the weak 1155 cm^{-1} solvent band. Thus, it is possible that our failure to observe much CT-resonant intensity in vibrations assignable to the C−Si stretch is simply a result of the "delocalization" of this bond stretch over multiple normal modes, along with experimental limitations that prevent us from observing all possible resonance enhanced vibrations. For comparison, the best-fit value of $\Delta = 1.05$ in the 1554 cm^{-1} TCNE C═C stretch (close to the $\Delta = 0.94$ we previously obtained in the hexamethylbenzene/TCNE complex)[28] would correspond to a bond length change of 0.063 Å in the quasidiatomic limit, only slightly smaller than the recently published theoretical value of 0.080 Å.[47]

If a significant change in structure and/or charge distribution does occur upon relaxation of the vertically excited ion pair to the relaxed, solvent-separated radical cation, how might that change arise? One possibility is that an electronic radiationless transition of some type occurs. A second possibility is that the global potential energy surface (which includes solvent coordinates) is significantly anharmonic such that the geometry changes in the silane group do not occur until the phenyl ring has distorted and/or the solvent has partially reorganized around the new charge distribution. In particular, rotation about the Ph−CH_2 bond might significantly modify the electronic communication between the phenyl and silyl groups. The DFT calculations, however, predict that the neutral and the radical cation have identical equilibrium $C_4-C_5-C_8-Si$ and $C_6-C_5-C_8-Si$ dihedral angles (refer to Figure 8) to within 1°. Brouwer and coworkers have shown that the excited-state geometry inferred from the local slope upon vertical excitation can be vastly different from the true relaxed geometry because of anharmonicities induced by avoided surface crossings,[21] although this does not appear to be a general feature of charge-transfer excited states.[23]

The agreement between the unscaled vibrational frequencies obtained from the DFT calculations and the experimental frequencies appears, in general, remarkably good for both the neutral and the radical cation. Of course, this molecule has a very large number of vibrations, all nominally Raman-allowed, of which we observe only a small subset, so finding a calculated frequency that closely matches any given experimental frequency is not difficult. However, the ^{13}C shifts place stringent additional constraints on the assignment of calculated to experimental frequencies for the modes of interest in this study. Many of the experimental frequencies have one or more calculated modes that are closer in absolute frequency than those assigned in Table 3, but these are clearly incorrect assignments based on the ^{13}C shifts. Even so, the rms error between experimental and calculated frequencies is a fairly impressive 19 cm^{-1} for the six assigned vibrations of the neutral and 18 cm^{-1} for the five assigned vibrations of the radical cation. The level of agreement between calculated and experimental vibrational frequencies provides reasonable confidence in the accuracy of the DFT calculated geometry changes upon oxidation summarized in Figure 8.

The experiments presented here probe only the initial and final states in the structural and/or electronic relaxation of **1** and **2** upon removal of an electron. Explicitly time-resolved measurements of various spectroscopic observables (absorption, emission, anisotropy, Raman, etc.) might help to provide a more complete picture of how the vertically excited state probed in the charge-transfer resonant Raman experiments evolves to the relaxed radical cation observed in the pump−probe experiments.[48−52]

Conclusions

To our knowledge this represents the first time vibrational information has been obtained for both the vertically (charge-transfer) excited and the relaxed forms of an organic radical ion. The results suggest that charge-transfer excitation of the *p*-methoxybenzyltrimethylsilane/TCNE ground-state complex involves removal of electron density primarily from the aryl ring system of the silane donor, whereas the relaxed silane radical cation probed tens of nanoseconds later has the hole localized mainly on the silane group. The reasons for this change in charge distribution upon ion-pair separation and vibrational and solvent relaxation remain to be determined. The good agreement between experimental and density functional theory calculated vibrational frequencies of the neutral and radical cation forms suggests that the calculated bond length changes of +0.10 Å in the benzyl C−Si bond length and −0.06 Å in the C−phenyl bond are reasonably reliable. The calculated lengthening and weakening of the C−Si bond is qualitatively consistent with the observed high reactivity toward nucleophilic cleavage of this bond upon oxidation.

Acknowledgment. This work was supported through the Center for Photoinduced Charge Transfer (NSF grant CHE-9120001). We thank Professor Joseph P. Dinnocenzo and members of his group for assistance in preparing the silane compounds and for helpful discussions on their chemistry.

References and Notes

(1) Myers, A. B.; Mathies, R. A. Resonance Raman intensities: A probe of excited-state structure and dynamics. In *Biological Applications of Raman Spectroscopy*; Spiro, T. G., Ed.; Wiley: New York, 1987; Vol. 2; p 1.

(2) Myers, A. B. Excited electronic state properties from ground-state resonance Raman intensities. In *Laser Techniques in Chemistry*; Myers, A. B., Rizzo, T. R., Eds.; Wiley: New York, 1995; p 325.

(3) Myers, A. B. *Chem. Rev.* **1996**, *96*, 91.

(4) Hudgins, D. M.; Allamandola, L. J. *J. Phys. Chem.* **1995**, *99*, 3033.

(5) Tang, W.; Zhang, X.-L.; Bally, T. *J. Phys. Chem.* **1993**, *97*, 4373.

(6) Szczepanski, J.; Auerbach, E.; Vala, M. *J. Phys. Chem. A* **1997**, *101*, 9296.

(7) Jeanmaire, D. L.; Suchanski, M. R.; Van Duyne, R. P. *J. Am. Chem. Soc.* **1975**, *97*, 1699.

(8) Keszthelyi, T.; Wilbrandt, R.; Cave, R. J.; Johnson, J. L. *J. Phys. Chem.* **1994**, *98*, 563.

(9) Ernstbrunner, E. E.; Girling, R. B.; Grossman, W. E. L.; Hester, R. E. *J. Chem. Soc., Faraday Trans. 2* **1978**, 501.

(10) Jeevarajan, A. S.; Kispert, L. D.; Chumanov, G.; Zhou, C.; Cotton, T. M. *Chem. Phys. Lett.* **1996**, *259*, 515.

(11) Sasaki, Y.; Hamaguchi, H. *Spectrochim. Acta* **1994**, *50A*, 1475.

(12) Brouwer, A. M.; Wilbrandt, R. *J. Phys. Chem.* **1996**, *100*, 9678.

(13) Tripathi, G. N. R.; Su, Y.; Bentley, J.; Fessenden, R. W.; Jiang, P.-Y. *J. Am. Chem. Soc.* **1996**, *118*, 2245.

(14) Dockery, K. P.; Dinnocenzo, J. P.; Farid, S.; Goodman, J. L.; Gould, I. R.; Todd, W. P. *J. Am. Chem. Soc.* **1997**, *119*, 1876.

(15) Myers, A. B.; Trulson, M. O.; Mathies, R. A. *J. Chem. Phys.* **1985**, *83*, 5000.

(16) Ci, X.; Myers, A. B. *Chem. Phys. Lett.* **1989**, *158*, 263.

(17) Gustafson, T. L.; Roberts, D. M.; Chernoff, D. A. *J. Chem. Phys.* **1984**, *81*, 3438.

(18) Hamaguchi, H.; Kato, C.; Tasumi, M. *Chem. Phys. Lett.* **1983**, *100*, 3.
(19) Hester, R. E.; Matousek, P.; Moore, J. N.; Parker, A. W.; Toner, W. T.; Towrie, M. *Chem. Phys. Lett.* **1993**, *208*, 471.
(20) Qian, J.; Schultz, S. L.; Bradburn, G. R.; Jean, J. M. *J. Phys. Chem.* **1993**, *97*, 10638.
(21) Brouwer, A. M.; Svendsen, C.; Mortensen, O. S.; Wilbrandt, R. *J. Raman Spectrosc.* **1998**, *29*, 439.
(22) Baker, K. V.; Brown, J. M.; Hughes, N.; Skarnulis, A. J.; Sexton, A. *J. Org. Chem.* **1991**, *56*, 689.
(23) Lilichenko, M.; Tittelbach-Helmrich, D.; Verhoeven, J. W.; Gould, I. R.; Myers, A. B. *J. Chem. Phys.* **1998**, *109*, 10958.
(24) Benesi, H. A.; Hildebrand, J. H. *J. Am. Chem. Soc.* **1948**, *70*, 3978.
(25) Foster, R. *Molecular Complexes*; Crane, Russak and Co., Inc.: New York, 1974.
(26) Conners, K. A. *Binding Constants: The Measurement of Molecular Complex Stability*; Wiley: New York, 1987.
(27) Markel, F.; Ferris, N. S.; Gould, I. R.; Myers, A. B. *J. Am. Chem. Soc.* **1992**, *114*, 6208.
(28) Kulinowski, K.; Gould, I. R.; Myers, A. B. *J. Phys. Chem.* **1995**, *99*, 9017.
(29) Kulinowski, K.; Gould, I. R.; Ferris, N. S.; Myers, A. B. *J. Phys. Chem.* **1995**, *99*, 17715.
(30) Myers, A. B.; Li, B.; Ci, X. *J. Chem. Phys.* **1988**, *89*, 1876.
(31) Trulson, M. O.; Mathies, R. A. *J. Chem. Phys.* **1986**, *84*, 2068.
(32) Gould, I. R.; Farid, S. *Acc. Chem. Res.* **1996**, *29*, 522.
(33) Haselbach, E.; Vauthey, E.; Suppan, P. *Tetrahedron* **1988**, *24*, 7335.
(34) Dombrowski, G.; Dockery, K. P.; Goodman, J. L.; Dinnocenzo, J. P.; Farid, S.; Gould, I. R., unpublished results.
(35) Frisch, M. J.; Trucks, G. W.; Schlegel, H. B.; Gill, P. M. W.; Johnson, B. G.; Robb, M. A.; Cheeseman, J. R.; Keith, T. A.; Petersson, G. A.; Montgomery, J. A.; Raghavachari, K.; Al-Laham, M. A.; Zakrzewski, V. G.; Ortiz, J. V.; Foresman, J. B.; Cioslowski, J.; Stefanov, B. B.; Nanayakkara, A.; Challacombe, M.; Peng, C. Y.; Ayala, P. Y.; Chen, W.; Wong, M. W.; Andres, J. L.; Replogle, E. S.; Gomperts, R.; Martin, R. L.; Fox, D. J.; Binkley, J. S.; Defrees, D. J.; Baker, J.; Stewart, J. P.; Head-Gordon, M.; Gonzales, C.; Pople, J. A. *Gaussian 94*, Revision C.3; Gaussian, Inc.: Pittsburgh, PA, 1995.
(36) Martin, J. M. L.; Van Alsenoy, C. GAR2PED; University of Antwerp, 1995.
(37) XMol; 1.3.1 ed.; Network Computing Services, Inc.: Minneapolis, MN, 1993.
(38) Frey, J. E.; Aiello, T.; Beaman, D. N.; Combs, S. D.; Fu, S.; Puckett, J. J. *J. Org. Chem.* **1994**, *59*, 1817.
(39) Nestor, J. R.; Lippincott, E. R. *J. Raman Spectrosc.* **1973**, *1*, 305.
(40) Eysel, H. H.; Bertie, J. E. *J. Raman Spectrosc.* **1988**, *19*, 59.
(41) Varsanyi, G. *Assignments for vibrational spectra of seven hundred benzene derivatives*; Wiley: New York, 1974.
(42) Durig, J. R.; Natter, W. J.; Johnson-Streusand, M. *Appl. Spectrosc.* **1980**, *34*, 60.
(43) Badger, R. M. *J. Chem. Phys.* **1934**, *2*, 128.
(44) Badger, R. M. *J. Chem. Phys.* **1935**, *3*, 193.
(45) Weisshaar, J. C. *J. Chem. Phys.* **1989**, *90*, 1429.
(46) Cuff, L.; Kertesz, M. *J. Chem. Phys.* **1997**, *106*, 5541.
(47) Juanós i Timoneda, J.; Peters, K. S. *J. Phys. Chem.* **1996**, *100*, 16864.
(48) Asahi, T.; Mataga, N. *J. Phys. Chem.* **1991**, *95*, 1956.
(49) Wynne, K.; Galli, C.; Hochstrasser, R. M. *J. Chem. Phys.* **1994**, *100*, 4797.
(50) Pullen, S.; Walker, L. A., II.; Sension, R. J. *J. Chem. Phys.* **1995**, *103*, 7877.
(51) Lenderink, E.; Duppen, K.; Everdij, F. P. X.; Mavri, J.; Torre, R.; Wiersma, D. A. *J. Phys. Chem.* **1996**, *100*, 7822.
(52) Kimura, Y.; Takebayashi, Y.; Hirota, N. *J. Chem. Phys.* **1998**, *108*, 1485.